Instability and Wavelength Selection during Step Flow Growth of Metal Surfaces Vicinal to fcc(001)

M. Rusanen,[1] I. T. Koponen,[2] J. Heinonen,[1] and T. Ala-Nissila[1,3]

[1]*Helsinki Institute of Physics and Laboratory of Physics, Helsinki University of Technology, P.O. Box 1100, FIN-02015 HUT, Espoo, Finland*

[2]*Department of Physics, University of Helsinki, P.O. Box 9, FIN-00014 Helsinki, Finland*

[3]*Department of Physics, Brown University, Providence, Rhode Island 02912-1843*

(Received 14 November 2000)

We study the onset and development of ledge instabilities during growth of vicinal metal surfaces using kinetic Monte Carlo simulations. We observe the formation of periodic patterns at [110] close packed step edges on surfaces vicinal to fcc(001) under realistic molecular beam epitaxy conditions. The corresponding wavelength and its temperature dependence are studied in detail. Simulations suggest that the ledge instability on fcc$(1, 1, m)$ vicinal surfaces is controlled by the strong kink Ehrlich-Schwoebel barrier, with the wavelength determined by dimer nucleation at the step edge. Our results are in agreement with recent continuum theoretical predictions, and experiments on Cu(1,1,17) vicinal surfaces.

DOI: 10.1103/PhysRevLett.86.5317 PACS numbers: 68.35.Fx, 68.55.–a, 81.15.Hi

In surface growth under molecular beam epitaxy (MBE) conditions, one of the central processes that controls the morphology of the surface is mass transport between growing layers. In homoepitaxial growth, there is usually an additional energy barrier controlling the interlayer transitions, known as the Ehrlich-Schwoebel (ES) or step edge barrier [1]. It plays a central role in stabilization of certain growing crystalline facets and eventually leads to growth of moundlike structures with a dynamically selected slope and length scale [2]. The influence of an interlayer ES barrier on growth has been extensively studied and its role on growth is now well understood [3,4].

However, recently it has been realized that in $1 + 1$ dimensional ledge growth corresponding to step-flow geometry, there is an analogous phenomenon which is due to the additional *kink Ehrlich-Schwoebel energy barrier* for going around a kink site at the step edge. The corresponding kink Ehrlich-Schwoebel effect (KESE) generated by it leads to the growth of a regular instability at step edge with a dynamically selected wavelength [5]. This is in contrast to the so-called Bales-Zangwill instability (BZI) [6] which tends to destabilize the 1D ledge morphology during growth because of terrace diffusion and step crossing, with no assumptions about line diffusion along the ledge. Ledge instabilities were originally found and reported experimentally on Cu(1,1,17) vicinal surfaces [7] but attributed to the BZI scenario. More recent experiments on the Cu(1,1,17) surface propose that the KESE instability may lead to formation of regularly shaped patterns with dynamical wavelength selection [8]. Recent theoretical studies of such instabilities suggest that KESE may indeed supersede BZI in the formation of growth patterns [5,9].

The growth of instabilities and wavelength selection have been studied recently within the framework of a continuum step model [5] and a simple solid-on-solid lattice model [9]. For the latter case, it has been demonstrated by kinetic Monte Carlo (KMC) simulations that KESE leads to the formation of wavy steps [9]. However, so far there is neither detailed knowledge of the actual structure of the patterns nor their dynamical evolution under realistic MBE conditions. The predictions of the continuum theory are mainly given in the weak KESE limit but they are not directly applicable in interpreting the experiments [5,10]. Namely, for simple metals such as Cu surfaces vicinal to fcc(001), at close packed step edges a strong KESE is expected. This is because theoretical estimates indicate barriers of the order of 0.5 eV for jumps around the kink site in the close packed [110] direction [11]. This is nearly twice the barrier of 0.26 eV for jumps along the straight step edge [11]. Based on the symmetry between the interlayer ES barrier which vanishes for [100] step edges [12], it is expected that the kink ES barrier vanishes for these orientations, too. Therefore, on surfaces vicinal to fcc(001) one should see a clear difference in unstable growth between the [100] steps and the [110] steps, the latter case being dominated by KESE.

In this Letter we present a detailed study of the growth and morphology of the steps on the Cu(1,1,17) surface vicinal to Cu(001). The model system used here is based on KMC simulations of a lattice-gas model [13] with energetics obtained from the effective medium theory (EMT) potential [11]. As discussed in detail in Ref. [11] the EMT barriers and their relative ordering is in good agreement with available experimental data for the Cu(001) surface. The intralayer hopping rate ν of an atom to a vacant nearest neighbor (NN) site can be well approximated by [11]

$$\nu = \nu_0 \exp[-\beta(E_S + \min(0, \Delta_{\mathrm{NN}})E_B], \qquad (1)$$

where the attempt frequency $\nu_0 = 3.06 \times 10^{12}\ \mathrm{s}^{-1}$ and the barrier for the jump of a single adatom is $E_S = 0.399$ eV. When there is at least one atom diagonally next to the saddle point the barrier is $E_S = 0.258$ eV. The change in bond number $-3 \leq \Delta_{\mathrm{NN}} \leq 3$ is the difference on the number of NN bonds between initial and final

states with bond energy $E_B = -0.260$ eV. The interlayer processes are also included in the model. Step crossing has a barrier of 0.58 eV from a straight edge and 0.44 eV through the kink site [11]. We note that within the EMT, barriers on the Ag(001) and Ni(001) surfaces are very similar to those of Cu(001) up to an overall scaling factor [11]. The geometry of the step edges with some of the pertinent single jump processes is shown in Fig. 1. The energetics of the model give a kink barrier of 0.518 eV for the [110] steps, and vanishingly weak KESE with a barrier of only 0.002 eV for the open [100] steps.

The KMC simulations were implemented using the algorithm by Bortz *et al.* [14] with a binary tree structure [15]. This allowed us to grow up to five monolayers (ML) of Cu under realistic temperature and flux conditions to study the development of unstable ledge patterns. The explored temperature range was $T = 240$–310 K and the flux $F = 3 \times 10^{-3}$–1.0 ML/s. Thus the ratio between the terrace diffusion and the deposition flux $D/F \approx 6 \times 10^5$–$9 \times 10^7$ in units of the lattice constant $a = 0.255$ nm, corresponding to a typical MBE regime [16]. System sizes considered consisted of eight terraces, each of width $L_x = 8.5$ and length up to $L_y = 2000$. With fully periodic boundary conditions there was a dependence of the selected wavelength on L_y. With open boundaries this dependence disappears, and in the ledge direction there was no difference in the results between $L_y = 500$ and $L_y = 1000$. However, periodic boundary conditions were necessary to study the temperature dependence of the structures, in which case we explicitly checked that this feature did not depend on L_y.

The choice of the initial conditions warrants some discussion. In principle, 1D step edges are thermally rough in equilibrium. Thus, we chose to start from initially rough step edges. We also performed some test runs starting from ideal, smooth ledges. In these cases development of the instability was much slower than when the steps were rough. We also discovered slight dependence of the characteristic wavelength of the instability on the initial condition. For both cases, however, we verified that the same temperature dependence was obtained.

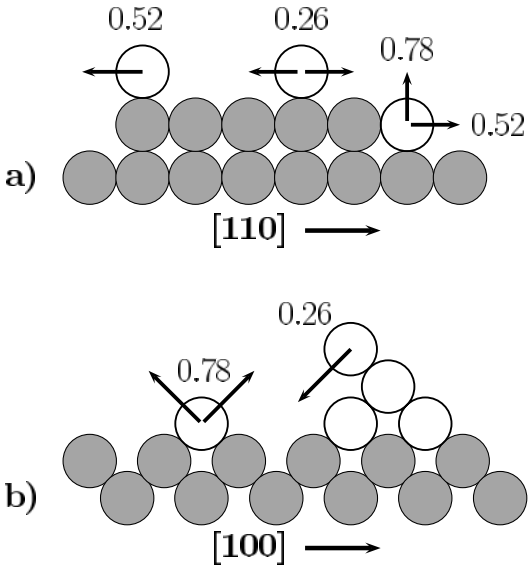

FIG. 1. Ledge geometry and some relevant single atom jump processes on (a) the close packed [110] step edge and on (b) the open [100] step edge. The energy barriers are given in eV.

We first show results for the step orientation [110] where KESE is relatively strong. In Figs. 2(a) and 2(b) there are step profiles after $\theta = 1.0$ and 5.0 monolayers, respectively, at $T = 240$ K with $F = 6 \times 10^{-3}$ ML/s. The development of an instability with a relatively well-defined wavelength for all ledges is apparent, and the steps seem to "phase lock" at the largest coverages studied. To quantify these results, we consider the lateral height correlation function for step edge profiles $\zeta(x, \theta) \equiv h(x, \theta) - \overline{h}(\theta)$, where h is the step height measured from $y = 0$ and $\overline{h}$ is its spatial average:

$$C(x, \theta) = \langle \zeta(x', \theta) \zeta(x + x', \theta) \rangle . \qquad (2)$$

Here, the brackets denote an average over the (deposition) noise and over all ledges in the system. The correlation function $C(x, \theta)$ for the [110] step edges at $T = 270$ K with $F = 6 \times 10^{-3}$ ML/s is shown in Fig. 3 for $\theta = 0.4$, 1.0, and 2.0, and its Fourier components are shown in the inset. The first minimum of $C(x, \theta)$ gives a measure of the characteristic length scale $\lambda \approx 37$ nm in the system and, as can be seen from Fig. 3, it is almost independent of θ even for coverages below the apparent phase locking. The same information is contained in the Fourier components of ξ. The arrow in Fig. 3 shows an estimate of the average distance between the growing fingers, as obtained directly from the ledge configurations. We note that in experiments the stabilization and phase correlation of the perturbations seems to improve between 5 to 50 ML [8]. Because of computational restrictions we have not been able to probe this regime, however.

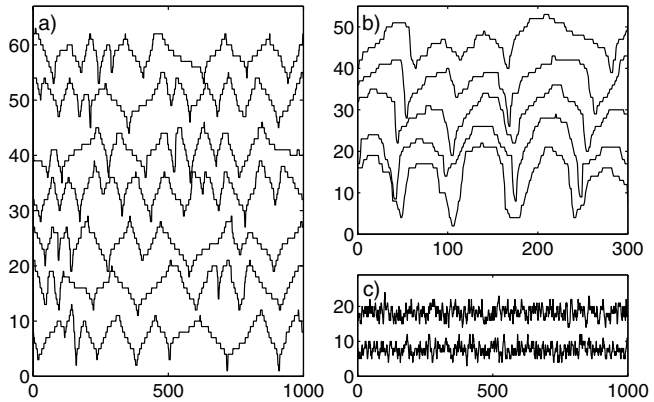

FIG. 2. Snapshots of typical step edge profiles with step orientations in the (a) and (b) [110] and (c) [100] directions at $T = 240$ K with $F = 6 \times 10^{-3}$ ML/s for coverages $\theta = 1.0$, 5.0, and 4.0, respectively. In the latter case KESE vanishes and the instability is strongly suppressed. The lateral and vertical scales are given in units of the lattice constant.

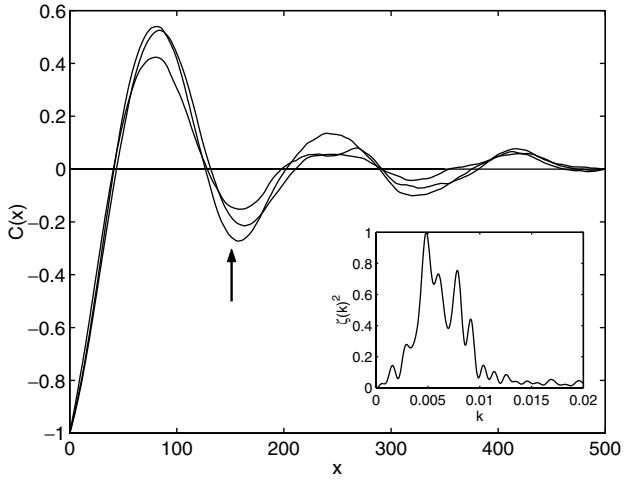

FIG. 3. The correlation function $C(x, \theta)$ for step edge fluctuations along the [110] ledge, for coverages $\theta = 0.4$, 1.0, and 2.0 at $T = 270$ K. The corresponding Fourier components of ζ are shown in the inset. An estimate for the wavelength obtained from the average distances between fingers is denoted by an arrow.

In Fig. 2(c) we show some step profiles for the open [100] steps after $\theta = 4.0$ monolayers. The difference with respect to the close packed steps is striking. Within the accuracy of the data, we find no evidence of unstable growth but the ledge fluctuations appear completely random. This is strong evidence indicating that in the present case, the patterns on the [110] ledges are due to KESE and not by BZI. In the absence of KESE, enhanced edge diffusion along the sides of the steps here strongly suppresses fluctuations of the [100] ledges [cf. Fig. 1(b)].

Let us next consider the origin of the wavelength ($\lambda \approx 30$ nm at $T = 240$ K with $F = 6 \times 10^{-3}$ ML/s) observed for the [110] ledges. It is of the same order of magnitude as the wavelength obtained in the experiments [8]. According to continuum theory for KESE [5], there are two important length scales controlling step flow growth with KESE. They are denoted by ℓ_c for dimer nucleation on a straight step, and the kink Schwoebel length $\ell_s = \exp[(E_s - E_d)/k_BT] - 1$ [5], which is related to the energy barriers E_s and E_d for jumps around a kink site and along a straight edge, respectively. When $\ell_s \ll \ell_c$, the nucleation length can be estimated from the model of Politi and Villain [10] (see also Ref. [5]). However, for the [110] ledges, $\ell_s \simeq 10^4$ and $\ell_c \simeq 10^2$ around room temperature, which indicates that we must consider the opposite case of a strong KESE.

In the case of a strong KESE, a more appropriate estimate for the nucleation length ℓ_c is obtained by considering the probability for nucleation of dimers at straight step edges. In the limit of infinite KESE it has been shown that $\ell_c \sim (D_s/F_s)^{1/4}$ [17]. Here $D_s \propto \exp[-E_d/k_BT]$ is the diffusion coefficient along the straight ledge and $F_s = FL_x$ is the flux at the ledge. In the case of finite but large ℓ_s, the corresponding 1D diffusion equation with appropriate boundary conditions has been solved by Politi [18]. From his solution, assuming that ℓ_c is controlled by dimer nucleation at the bottom of the growing step structure gives $\ell_c = (12D_s/F_s)^{1/4}$. Since the width of the 1D terrace fluctuates between zero and ℓ_c [10], we obtain an estimate for the wavelength as

$$\lambda \approx \frac{1}{2}\left(\frac{12D_s}{F_s}\right)^{1/4}. \tag{3}$$

The scaling exponent 1/4 is a direct consequence of dimer nucleation at the ledge and is always expected for strong KESE within the present model. The relation in Eq. (3) predicts that the temperature dependence of λ is controlled by an effective barrier $E_{\text{eff}} = E_d/4$. In the present case this becomes about 65 meV. The estimate for E_{eff} in the case of BZI gives a value nearly an order of magnitude larger [8]. Equation (3) also predicts that $\lambda \sim F_s^{-\alpha}$ with $\alpha = 1/4$, in contrast to the BZI case where $\alpha = 1/2$ [6].

With the present energetics, Eq. (3) gives $\lambda \approx 40$ nm at $T = 270$ K with $F = 6 \times 10^{-3}$ ML/s, which is in very good agreement with the simulation result $\lambda \approx 37$ nm. This is in contrast to BZI which yields $\lambda \approx 1$ nm [8]. We have furthermore tested the predictions of Eq. (3) by estimating λ at different temperatures and also by varying the flux. In Fig. 4 we show the temperature dependence of λ for various temperatures in an Arrhenius plot. A straight line fit to the data gives $E_{\text{eff}} = 75 \pm 10$ meV, in good agreement with the prediction based on Eq. (3). This estimate is also in good agreement with the experimental result by Maroutian *et al.* [8]. In the inset in Fig. 4 we also show the flux dependence of λ and compare it with that obtained from Eq. (3) with no fitting

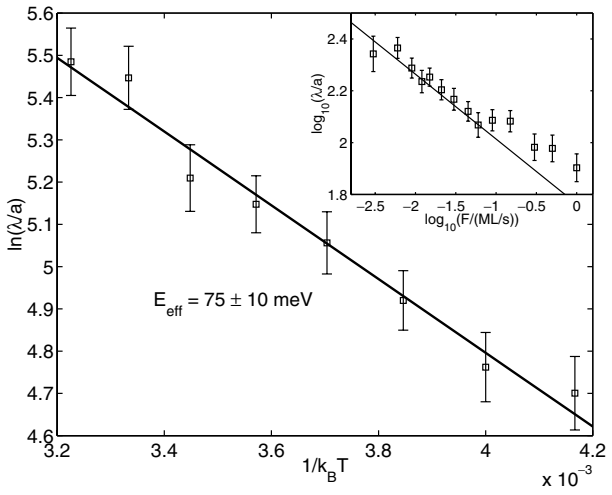

FIG. 4. Temperature dependence of the wavelength λ obtained from the distance between the fingers. It has been determined after deposition of 2.0 ML with $F = 6 \times 10^{-3}$ ML/s at $T = 240 - 310$ K. The least squares fit is shown by a continuous line with a slope denoted in the figure. In the inset the flux dependence of λ is shown at $T = 300$ K with fluxes $F = 3 \times 10^{-3} - 1.0$ ML/s after deposition of 2.0 ML. The straight line is the theoretical prediction of Eq. (3). For the highest flux values, there is indication of terrace nucleation.

parameters. We find excellent agreement between theory and simulations, except for the largest fluxes where terrace nucleation becomes apparent. Fitting to flux values up to $F = 9 \times 10^{-2}$ ML/s gives $\alpha = 0.23 \pm 0.03$.

Finally, we discuss the roughness of the step in terms of the width of the step edge fluctuations $w(\theta) = \sqrt{\langle \zeta(\theta)^2 \rangle}$. We find that $w(\theta)$ increases with coverage and does not show signs of saturation up to about 5 ML. Up to this region the width follows a power law behavior $w(\theta) \sim \theta^{\beta}$, with $\beta \approx 0.3$ as seen in the case of an isolated step [19]. The solid-on-solid model gives for strong KESE an exponent $\beta \approx 0.57$ [5], $\beta = 1$ has been obtained for a one-sided step growth model with an infinite kink barrier [20], while for a collection of steps in the phase-locking regime $\beta = 1/2$ [21]. This indicates that β depends on the details of the model for unstable growth and may also depend on the coverage regime considered.

To summarize, the general situation regarding 1D ledge instabilities under growth is a complicated one [4] (see also [19,20]). The simulations presented here give support to the view that on vicinal Cu$(1, 1, m)$ surfaces the observed instability is due to KESE. This means that the competing BZI is of no importance either in length and time scales studied here or in those accessed in the experiments. In our simulations we have been able to demonstrate the onset of the wavelength selection, in qualitative agreement with continuum theoretical predictions. Moreover, it was possible to connect the observed temperature dependence of wavelength to the underlying energetics. This is in qualitative agreement with experimental observations and theoretical predictions for strong KESE, and clearly incompatible with BZI. Simulations also confirm the crucial role of the dimer nucleation length in determining the length scale of the patterns. Although we cannot conclusively demonstrate the phase locking of the step fluctuations, there is evidence that this indeed occurs at higher coverages.

We thank T. Maroutian for providing us with unpublished data and M. Rost, J. Kallunki, and T. S. Rahman for useful comments. This work has been supported in part by the Academy of Finland through its Center of Excellence program.

[1] R. L. Schwoebel, J. Appl. Phys. **40**, 614 (1969).
[2] M. Siegert and M. Plischke, Phys. Rev. Lett. **73**, 1517 (1994); Phys. Rev. E **50**, 917 (1994).
[3] H.-C. Jeong and E. D. Williams, Surf. Sci. Rep. **34**, 171 (1999).
[4] P. Politi, G. Grenet, A. Marty, A. Ponchet, and J. Villain, Phys. Rep. **324**, 271 (2000).
[5] O. Pierre-Louis, M. R. D'Orsogna, and T. L. Einstein, Phys. Rev. Lett. **82**, 3661 (1999).
[6] G. S. Bales and A. Zangwill, Phys. Rev. B **41**, 5500 (1990).
[7] L. Schwenger, R. Folkerts, and H. J. Ernst, Phys. Rev. B **55**, R7406 (1997).
[8] T. Maroutian, L. Douillard, and H. J. Ernst, Phys. Rev. Lett. **83**, 4353 (1999); T. Maroutian (private communication).
[9] M. V. Ramana Murty and B. H. Cooper, Phys. Rev. Lett. **83**, 352 (1999).
[10] P. Politi and J. Villain, Phys. Rev. B **54**, 5114 (1996).
[11] J. Merikoski, I. Vattulainen, J. Heinonen, and T. Ala-Nissila, Surf. Sci. **387**, 167 (1997); J. Merikoski and T. Ala-Nissila, Phys. Rev. B **52**, R8715 (1995).
[12] U. Kürpick and T. S. Rahman, Phys. Rev. B **57**, 2482 (1998).
[13] J. Heinonen, I. Koponen, J. Merikoski, and T. Ala-Nissila, Phys. Rev. Lett. **82**, 2733 (1999).
[14] A. B. Bortz, M. H. Kalos, and J. L. Lebowitz, J. Comput. Phys. **17**, 10 (1975); M. Kotrla, Comput. Phys. Commun. **97**, 82 (1995).
[15] J. L. Blue, I. Beichl, and F. Sullivan, Phys. Rev. E **51**, R867 (1995).
[16] J. Krug, Adv. Phys. **46**, 139 (1997).
[17] J. Krug, J. Stat. Phys. **87**, 505 (1997).
[18] P. Politi, J. Phys. I (France) **7**, 797 (1997).
[19] T. Salditt and H. Spohn, Phys. Rev. E **47**, 3524 (1993).
[20] J. Heinonen, I. Bukharev, T. Ala-Nissila, and J. M. Kosterlitz, Phys. Rev. E **57**, 6851 (1998).
[21] O. Pierre-Louis, C. Misbah, Y. Saito, J. Krug, and P. Politi, Phys. Rev. Lett. **80**, 4221 (1998); J. Kallunki and J. Krug, Phys. Rev. E **62**, 6229 (2000).